THE AMERICAN SOCIETY OF MECHANICAL ENGINEERS
345 E. 47th St., New York, N.Y. 10017

96-GT-48

NUMERICAL AND EXPERIMENTAL INVESTIGATION OF A RICH QUENCH LEAN COMBUSTOR SECTOR

Johannes W. Koopman
Institute for Propulsion Technology
German Aerospace Research Establishment
Cologne, Germany

Peter Griebel
Christoph Hassa

ABSTRACT

The flow in a three sector model, representing a segment of an annular rich quench lean combustor for an aeroengine is investigated. Detailed knowledge of flow, temperature and species concentration distributions is of decisive importance to control the NOx formation, essential to the RQL concept. Velocities, temperatures and species concentrations are measured. They are partly used to aquire data on the inlet boundaries in the numerical calculation and partly used to compare with the numerical results. The calculation reveals many details which are not accesable in the experiment. It also shows the effects of the specific inlet dataset. Experimental data and numerical results furnish complementary information.

INTRODUCTION / MOTIVATION

The combustor concept with Rich-burn / Quick-quench / Lean-burn combustion appears to be one promising candidate to reduce NOx emission levels of aeroengines. The concept, originally conceived for industrial combustors, uses staged burning (Mosier et al., 1980), (Pierce.et al., 1990).

Combustion starts in the primary zone under fuel rich conditions at equivalence ratios between 1.3 and 2.3. NOx production is limited by the almost complete consumption of the available oxygen (as well as the tendency of unburned hydrocarbon radicals to reduce NO). Secondary air, cooling the primary zone, enters the combustor in the mixing sector, thereby decreasing the equivalence ratio to values between 0.35 and 0.45. Quick and complete mixing forms the key of the RQL-concept. In the secondary zone a balance between burnout and minimal NOx production has to be maintained. The geometric cross-section of the mixing zone usually has a smaller cross-section than the rich zone, in order to reduce the "communication" between the recirculating part of the rich primary zone mixture and the fresh jet air stream.

In the USA the RQL concept has been chosen as one of the technologies in the HSCT program (Shaw et al., 1993) to achieve a low environmental pollution level. In Germany the Motoren und Turbinen Union (MTU) Munich adopted the RQL concept in 1989. In a first step the emission reduction potential of a tubular combustor was investigated (Zarzalis and Ripplinger, 1992). Basic studies on two stage flows were performed by Knapp et al. (1993). The results stimulated the use and gained experience in a rectangular combustor sector representing an optically accessable approximation of an annular aircraft combustor. This configuration was investigated in the Low Emission Combustion Technology project of the research program of the European Commission in cooperation with European partners. It is the purpose of this research project to demonstrate the NOx-emission reduction potential of the RQL combustion under realistic operation conditions. In the cooperation between MTU and its research partners, MTU designed and manufactured a sector and performed tests up to 18 bars. The German Aerospace Research Establishment (DLR) built a second sector with identical geometry and optical access on both side walls. In this sector the flow field and the temperature and mixture distribution were measured under atmospheric conditions with conventional and laser techniques. The parallel investigation of mixture and reaction at 1 bar under realistic conditions was conducted to rationalize optimization of the combustor geometry (Griebel et al., 1995).

EXPERIMENTAL SETUP AND TECHNIQUES

Setup

Figure 1 shows a cross-section of the experimental setup seen from the side and the top. Air preheated to 850 K, is metered by critical nozzles in the inlet and divided in primary and secondary air. The kerosene fuel supply system is watercooled, fuel preparation is achieved by airblast nozzles. Swirling of the primary air causes a recirculation in the primary zone, stabilizing the diffusion flame. The

Presented at the International Gas Turbine and Aeroengine Congress & Exhibition
Birmingham, UK — June 10-13, 1996

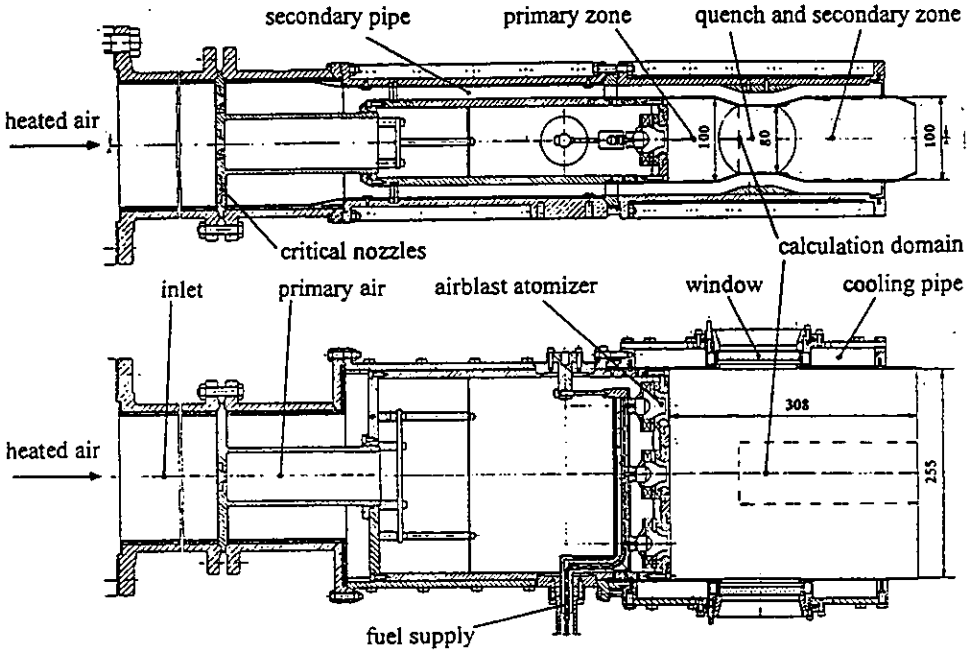

Fig. 1 Experimental Setup.

liner walls in the primary zone are convectively cooled with the secondary air, liner walls in the secondary zone are film cooled. In the mixture zone transparent windows are used to allow the use of optical measuring methods (LDA, CARS). A detailed description of the setup can be found in Lenze (1994). A perspective view of the geometry of the middle sector is shown in Fig 2. To inject the secondary air, four rows of holes on the top as well as on the bottom are used, where the holes on the top and bottom sides are exactly opposite of each other (in line), but the holes are shifted in the downstream direction (staggered).

Experimental techniques

Conventional techniques. Local gas composition was measured using suction probes (Lenze, 1994). We measured CO2, CO, H2, O2, NO (NOx), and UHC. The accuracy of the chemiluminesence NOx analyser for the fuel rich environments with equivalence ratio > 2, was improved by using a special heated converter and sufficient dilution with oxygen (Tuttle et al. 1974).

Temperatures were measured with a Al2O3 layered PtRh-Pt 30/6 Thermocouple. Measured temperatures were corrected for radiation.

Optical methods. LDA measurements were performed with TSI (model 9107 and 9155) optics and Dantec electronics (model BSA) in forward scattering. titaniumdioxid particles (< 1 mm) were added to the preheated air flow. The accuracy of the averaged velocities can be estimated with 5 %.

NUMERICAL METHOD

Code

In order to simulate the fluid mechanical and chemical processes in the combustor an unstructured 3D Navier-Stokes code "TRUST", developed at the DLR for the use in gasturbines and based on the KIVA II code of Amsden et al. (1989) has been used. The time dependent conservation equations for the turbulent flow of a chemical reacting mixture of ideal gases are solved. These are discretized with the finite volume approximation on a three dimensional grid of contour fitted hexahedrons with cartesian coordinates. The special ALE-solver (Arbitrary Lagrange Eulerian Method) performes well on reacting flows.

The half empirical k-ε model is used to model the correlations of the velocity fluctuations as they arise by the time averaging of the Navier-Stokes equations. For turbulent reacting flows, fluctuations of density, temperature and composition can dominate their average counter parts. Consequentely we need to describe apart from the forementioned turbulence model, approximations the influence of turbulence on chemical reactions.

Combustion model

In the combustion model used the species reaction time scale is thought to be very small compared to the turbulent time scale, such that mixture can be considered to be in chemical equilibrium. The transport of the species mass fractions is dominated by the turbulent flow field and is characterized by the transport of the mixture fraction $\bar{f}$ and its fluctuating counterpart $g = f''^2$. The discretisation process, basic to many numerical codes, applies the assumption that in a small volume (cell) properties are constant for a small time step. So the chemical state of the mixture can be descibed by the equilibrated mixture and its energy level. However in the small timestep considered, turbulence influences the mixture and the energy, such that a number of equilibrium states in each volume exists. This time dependent behaviour can be described by probability density functions, which give the distribution in time of all possible states. Because we are looking at stationary flows, the underlying assumption that the resulting "stationary" time distribution is the superposition of all "small-timestep" time distributions is reasonable. In this work the Beta distibution is used.

Grid

The CFD calculation domain comprises the central third of the flame tube, beginning at the end of the primary zone, see Fig. 1. On each sector secondary air is injected through 4 rows of 10 - 10 - 10 - and 11 holes. Hole diameter and spacing have been chosen such that

optimum mixing could be expected. Every hole was represented by grid nodes (4 cells). Four rows of cooling holes on the top as well as the bottom sides were represented by 4 cooling slots, so that a total of 95 inlets for each section had to be considered. The quick and complete mixing forms the key of the RQL concept, special emphasis was laid upon the mixing technique and the calculations were restricted to the mixing and secondary zone of the idealized sector. The resulting grid had 80 x 31 x 61 node points.

Boundary conditions

In Fig. 2 a perspective upstream view of the geometry of the middle sector shows the inlet configuration used. As discussed in the next chapter of this paper the air and fuel mass flows have been chosen by

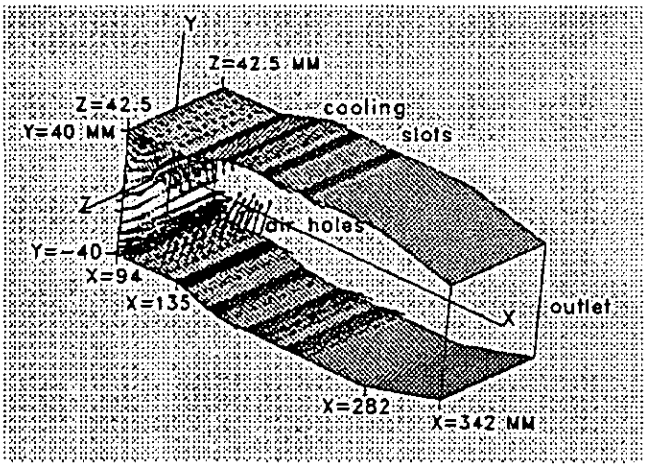

Fig. 2 Geometry of the Sector with Inlet Flows Vectors

the experiment to give a minimal NOx emission index at the combustor exit.

Mixing zone inlet. The calculations started in the entrance plane of the mixing zone (= exit plane of the primary zone) with measured velocity, temperature and composition distributions.

The number of measured points was small (typical 5 x 5) compared to the number of grid entrance points (typical 60 x 30). Moreover the measured distributions did not completely show the expected periodicity, which is necessary for the calculation. In the interpolation process used periodicity was enforced.

Due to limited optical access only the axial and vertical velocity components were measured. An inclined view on the axial-vertical vector plot (Fig. 3) reveals however the entering flow probably has at least one vortex system, with its axis pointed downstream. A more detailed discusion follows in the next chapter of this paper.

The turbulence energy level was estimated from the measured rms values of the axial and vertical velocity components. Based on earlier

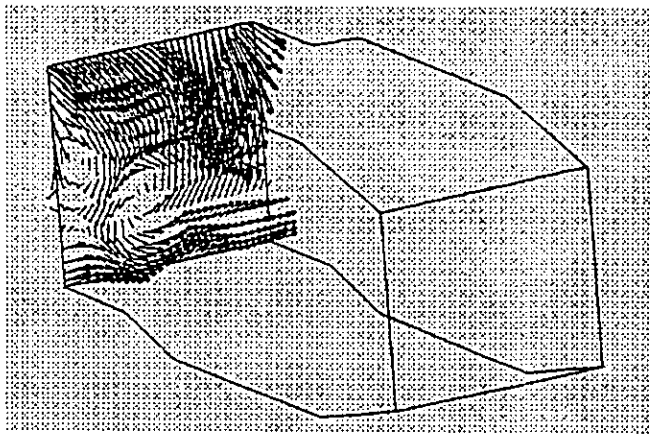

Fig. 3 Perspective View of Axial-Vertical Velocity Vector

measurements in simular geometries, the turbulence length scale, which was not measured, was taken to be 1 mm.

	quench row			
Row number	1	2	3	4
No of holes	11	10	10	11
Hole diam. (mm)	4.1	4.5	4.4	3.7
Air mass flow (%)	11	14	13	11
jet angle (deg)	63	67	72	77
	film row			
Row number	1	2	3	4
Air mass flow (%)	7	7	8	7

Table 1 Massflow Distributions and Jet Angles of Secondary Air Holes and Film Cooling

Mixing holes and cooling slots. Air enters with a temperature of 850 K through the mixing holes and the film cooling slots. The present calculation represents an intermediate step, in which the modeling of the secondary channel was not yet realized. Thus the relative air mass flows and jet angles described in Table 1, as given by MTU are used. Again only two velocity components can be estimated. Air flow through the cooling slots was given a small vertical component, such that no unrealistic penetration could be expected.

Exit boundary. The exit boundary only showed outflow. In KIVA diffusive fluxes on the exit boundary are set zero. If pressure is described on an outflow boundary, pressure waves are reflected because outlet pressure is not known a prioi. Therefore pressure

follows from a specified ambient pressure at a prescribed distance, which then gives a linear weighted average of and a zero gradient and a prescibed pressure condition. This technique was found to be necessary to suppress unphysical pressure fluctuations.

Combustor wall. The combustor wall was taken to be adiabatic (zero enthalpy gradient). Wall stresses were estimated with the usual wall function approaches.

Transverse boundaries. The primary zone flow in all three sectors was co rotating, so that for the center sector periodical (cyclic) boundaries had to be assumed.

COMBUSTOR FLOW

Mass flows

To optimize the total and primary zone air distribution, we identified the condition with the minimum TFN production. TFN (Total Fuel Nitrogen) is the sum of all nitrogen containing species, mainly NO, NO2, HCN and NH3. The TFN was established by chemical conversion of NO2 into NO and almost complete conversion (80 - 90 %) of HCN and NH3 into NO during the NOx measurement. In this way the measured NOx concentration corresponds with the TFN concentration. Fig. 4 shows the mass averaged dimensioneless emission index EINOx (g NOx/kg fuel) at the combustor resp. the primary zone outlet as a function of the total resp. primary zone equivalence ratio. In the combustor exit plane a minimal EINOx index of 3.35 g NOx/kg fuel is attained for a total air number of 0.35. The corresponding primary zone equivalence ratio is 2.13. For large primary zone air numbers (> 2.13) the EINOx declines because the convertion of HCN and NH3 into NO decreases strongly, such that the gained NOx values do not represent the TFN values anymore.

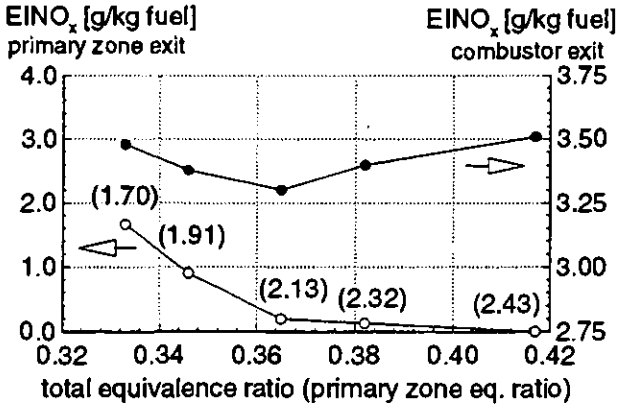

Fig. 4 EINOx as a Funktion of the Total resp. the Primary Zone Equivalence Ratio

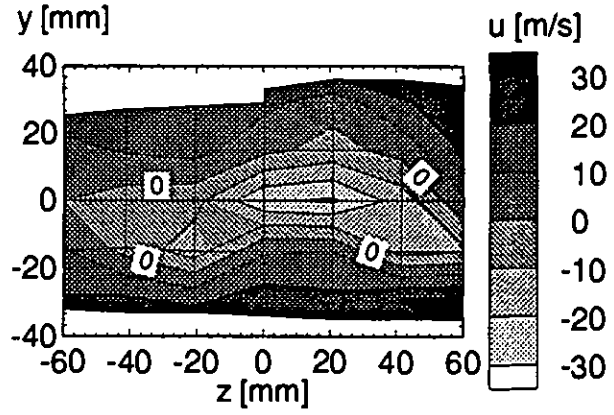

Fig. 5 Measured Axial Velocity Distribution at Primary Zone Exit

Inlet boundary flow

The flow entering the mixing zone is determined by its history in the primary zone. Looking upstream the flow in all three sectors is swirling clockwise. In a rectangular cross-section corner vortices rotating counterclockwise will fill out the spaces not occupied by the swirling flows from the nozzles. Because of the interaction with the sidewalls, the aerodynamic centerlines of the outer nozzle flows are deflected in the counter clockwise direction. Hence, the counter rotating vortices also move in the same direction, causing the lower left corner vortex in the entrance plane of the calculation domain to move into the middle sector, as seen on the lower left of Fig. 3. It can

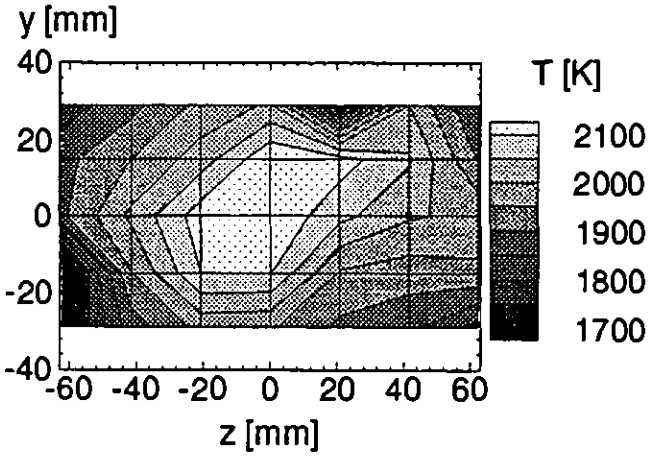

Fig. 6 Measured Temperature Distribution at Primary zone Exit

also be observed, that the inlet flow on the upper right side is mainly pointing downwards. It is likely that this is caused by an interaction with the secondary mass flow.

Measurements of the jet velocities showed that the secondary mass flow was not distributed fully homogeneous in the azimuthal (z) direction. Fig. 5 shows isolines of the axial velocity component. It can

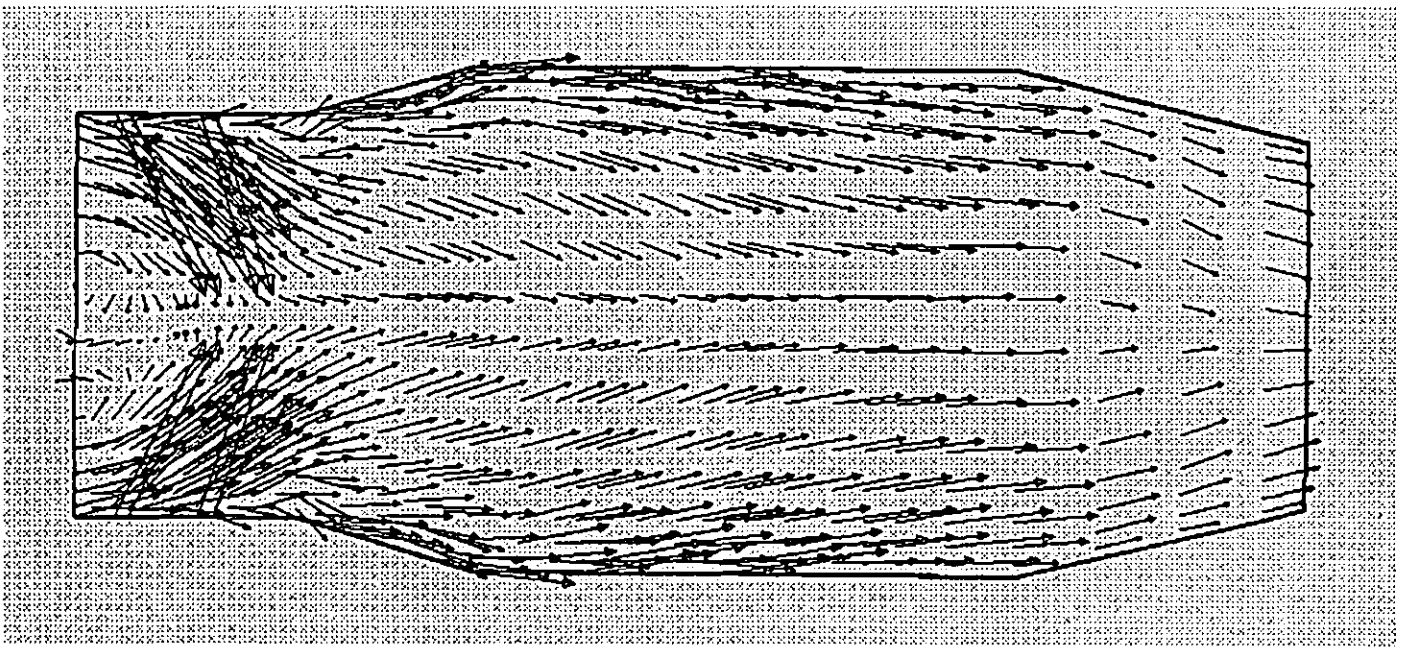

Fig. 7 Flow Vectors in Axial-Vertical Midplane (z=-4 mm)

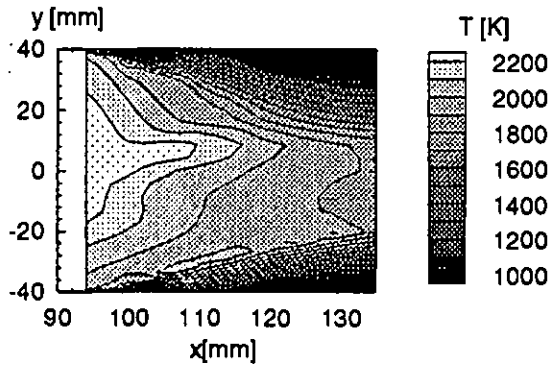

Fig. 8 Calculated Temperature Distributions in Axial-Vertical Mid-Plane (z=-4mm)

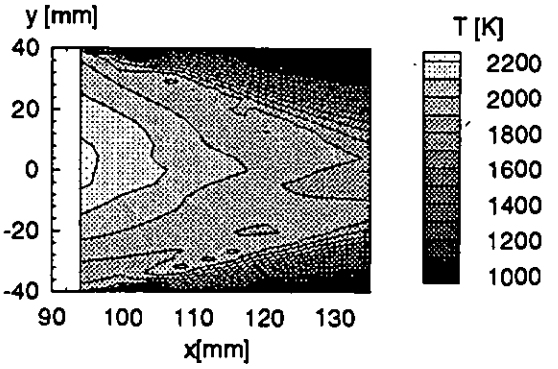

Fig. 9 Calculated Temperature Distributions in Axial-Vertical Edge-Plane (z=-38mm)

be observed, that a backflow exists from the mixing zone to the primary zone, however the strongest backflow is not positioned central, as was expected. Nevertheless Fig 6. shows that the temperature distribution in the plane is shifted in the opposite direction as the backflow, indicating that maximum exchange between primary zone flow and fresh jet air does not coincide with the maximum primary zone backflow, which is supplied in part by the strongly downturning primary zone flow on the upper right side of Fig 3, not providing additional oxygen for the rich mixture.

Mixing and secondary zone flow

Fig. 7 shows an axial-vertical view in a cross-section situated almost in the middle of the sector (z=-4 mm), through a first, a third and a fourth row hole. The jet inflow angles are as suggested by MTU. Because the backflow is strongest in the middle area of the sector, the momentum ratio of the jet to primary zone flow reaches a maximum here and the jets penetrate faster to the middle plane than in the left sector boundary. Here the vertical movement of the jets is preserved well into the secondary zone. Nevertheless insufficient penetration of the jets can be obeserved and consequently a hot core extends into the secondary zone, as it can be seen in the corresponding temperature maps in Fig. 8 and Fig. 9.

The flow in the central region doesn't convectively exchange with the outer regions. Moreover, the level of turbulence shown in Fig 10 decreases very rapidly after jet penetration with the consequence that turbulent exchange between the central and the outer regions can be

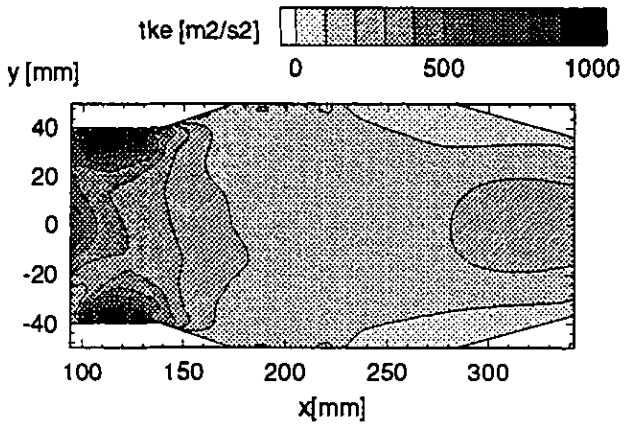

Fig. 10 Distribution of the Turbulent Energy in Axial-Vertical Midplane (z=-4 mm)

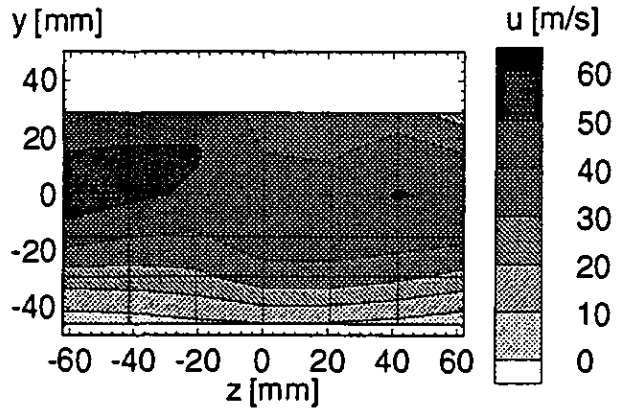

Fig. 11 Measured Distribution of the Axial Velocity Component in

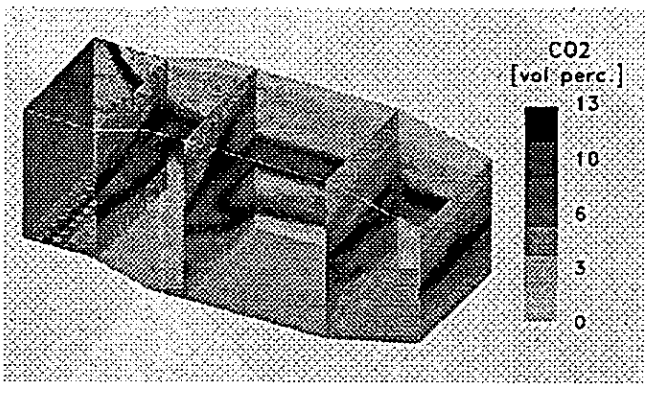

Fig. 12 Perspective View of CO2 Distribution

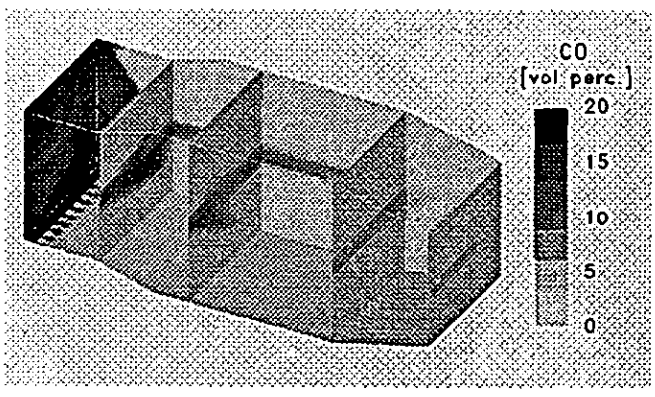

Fig. 13 Perspective View of CO Distribution

neglected. The measured axial velocity distribution of Fig. 5 shows unfavourable backflow in the center of the exit plane of the primary zone, thus potentially connecting fresh jet air with rich primary zone gas. Hence the primary zone mixture will be less rich, causing the temperature to rise, which probably leads to an increase of the highly temperature dependent NOx productability. The observed jet under penetration attenuates the backflow tendency. This might be reponsible for the remarkably low NOx emission index (3.35 g NOx/ kg fuel) of the sector. Overpenetrating jet flows, colliding in the center would obstruct the primary zone flow, thus causing enhancement of present backflow.

The calculated combustor outflow profiles still reflect the primary zone inhomogeneities, whereas the measured distribution of Fig. 11 shows no structure in the azimuthal (z) direction. Apparently the primary zone and the mixing zone horizontal mass flow variation of the experiment cancel each other to a certain extent. The resulting CO2 distribution as shown in Fig. 12 therefore shows a downstream layered maximum in the central region. As discussed in the next chapter the CO content decreases downstream (Fig 13), but has its maximum in the central region.

The rich primary zone flow is composed of a mixture nf completely reacted species, such as CO2 and H2O, and partially reacted species, such as CO, OH and H2. By mixing it with fresh air the CO2 and H2O content first will increase by reaction and then decrease by excess air dilution. The primary zone mixture partially mixes with the jet flow and reacts. Some of the mixture is deflected towards the central region and only reacts slowly, another part mixes quite well and reacts fast. Especially around the front edge of the first row nf jets fast and complete reaction takes place as can be seen in Fig 12, where a CO2 maximum locates the reaction zone.

A small part of the mixture flows around the roots of the jets. In Fig 14 the resulting H2O distribution in an axial-azimuthal half-plane near the bottom wall (H/D=.5) has been plotted. Increased reaction takes place between the jets, leading to an increase of H2O. The combustion products flow around the roots of the next row of holes, where the mixture becomes lean and the H2O content diminishes. The third and fourth jet rows transport the combustion products away

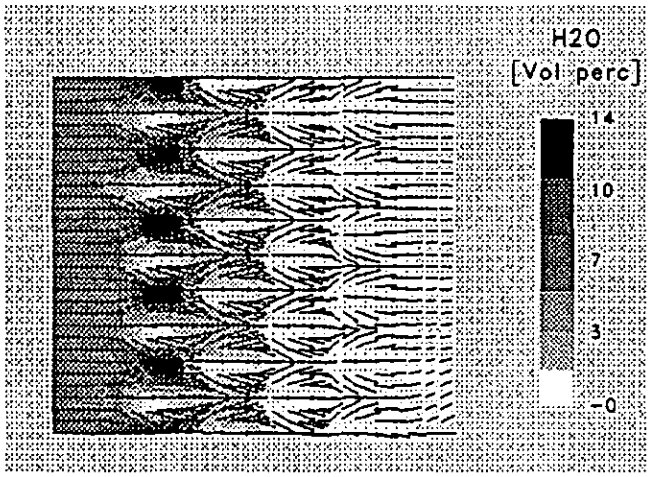

Fig . 14 Top View of H2O Distibution in Half-Plane near Bottom Wall of Quench Section at H/D=.5 (y=-38 mm)

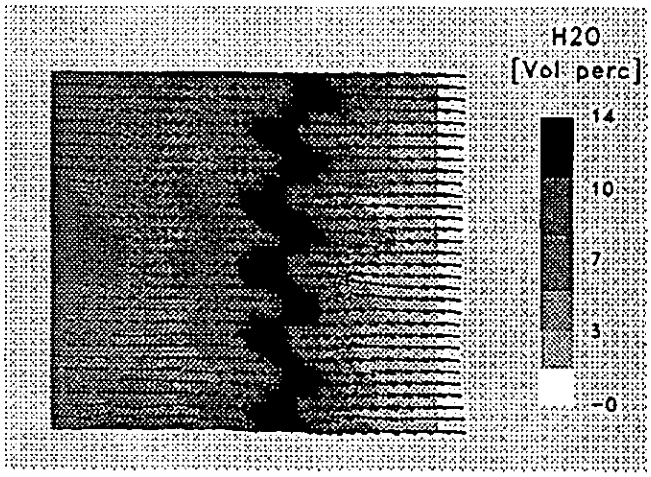

Fig . 15 Top View of H2O Distibution in Half Plane of Quench Section at H/D=4.45 (y=-22 mm)

from the wall. Allthough the grid was not fine enough to resolve a possible backflow downstream of the jet roots, it can be observed that the jet downstream area principally does not contain combustion products. Moreover the CO2 and CO concentration from Fig. 12 and Fig. 13 are very low in the vicinity of the walls. It appears that a relatively cold air layer exists, maintained by the film cooling air.

Observing a second plane (Fig. 15), situated higher above the bottom wall (H/D=4.45) we notice that the pattern of the first row of jets is still recognizable. The H2O maximum lies more downstream, which shows the jet deflection. The maximum now is connected, showing azimuthal mixing of the single jet flows.

Observation of composition in the central (higher) region shows an almost constant H2O content, indicating absence of reaction caused by the absence of jet air. The jets do not penetrate into the central region.

CALCULATION AND MEASUREMENTS

The calculations of the flow in the mixing and secondary zone used the measured temperatiure, velocity and species concentrations distributions of the primary zone exit plane (x=94mm). As discussed the flow in this plane was not completely periodic, the distributions seem to be shifted. We also observed that the secondary channel flow does not homogeneously split between the jet flow holes. The number of measurements however was not large enough, only in two axial-vertical planes, to allow a detailed prescription of velocity distributions in all 90 holes considered (including 8 half-holes). We therefore used azimuthal uniform, axial tabeled (Table 1) massflows suggested by MTU, without hole-based distributions.

The higher momentum ratio between jetflow and primary zone flow in the experiment relative to the calculation, leads to a higher penetration see Fig. 16 and Fig. 17. Moreover differences in the momentum of neighbouring jets generates turbulence and consequentely promotes turbulent exchange, which improves mixing.

The calculated temperature distribution of the mid-plane (z=-4mm) in the mixing zone (x=94 —> 135 mm) given in Fig. 8, is the consequence of the inlet conditions. The stronger experimental radial momentum in this plane forces the measured temperature isolines to be narrower than in the measurement of Fig. 16.

The distributions of the edge plane (z=-38mm), shown in Fig. 9, are less narrow, but show the same trends. Incomplete penetration and less azimuthal turbulent exchange cause the calculated temperatures of the central region of both planes considered of Fig. 8 and Fig 9 to decrease slower axially than the comparative measured temperatures in Fig. 16 and Fig. 17. A comparison of the velocity field in the same axial-vertical plane supports these conclusions and was hence deemed redundant.

The calculated CO2 distributions of Fig. 12 indicate a hot layer in the central region of the mixing and the secondary zone. Some primary zone mixture "survives " the mixing zone as we can see from the CO distributions of Fig. 13.

Although in the experiment the maximum CO concentration of 0.4 volume % can be found in the central region too, the experimental concentration level is considerable lower than the calculated level. MTU measuremets at 7 bars showed a further increased burnout (Zarzalis, 1995).

CONCLUSION

In this contribution, we demonstrate the potential and the limitations of a numerical calculation compared to the information given by the experiment in the case of a complex aeroengine combustor. Allthough the experiment furnishes an incomplete inlet boundary dataset, the calculation reveals many features of the flow, which are not apparent

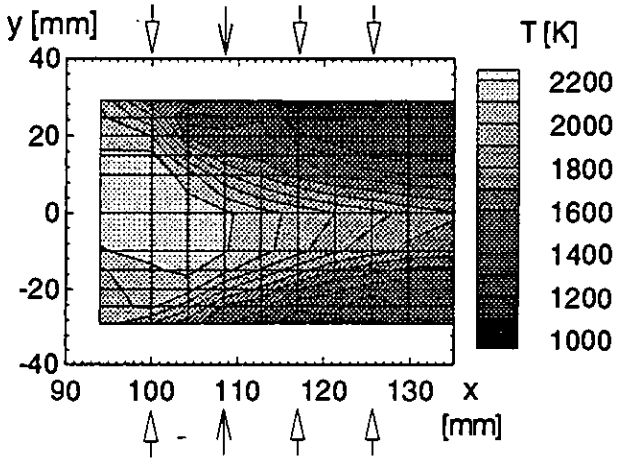

Fig. 16 Measured Temperature Distributions in Axial-Vertical Mid-Plane (z=-4mm)

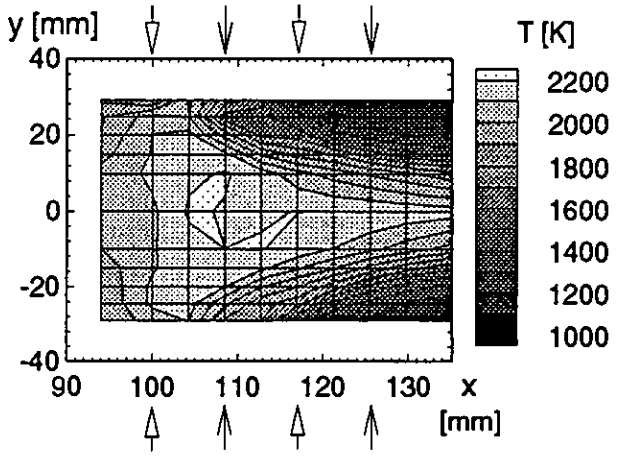

Fig. 17 Measured Temperature Distributions in Axial-Vertical Edge-Plane (z=-38mm)

in the experimental data, thus supporting the understanding of the process under study.

The combustor shows a remarkably low NOx emission index. Compared with a modern conventional combustor a 60 % reduction was achieved. Hence the investigation also shows, that the RQL method can be a comparatively robust method, which produces appreciable NOx reductions, even at non optimum flow conditions.

The described combined experimental numerical method will be used to develop a further mixing module (Migueis and Hassa, 1995), promising a still larger NOx-reduktion potental (Griebel et al. 1995).

ACKNOWLEDGMENTS

The authors wish to thank the European Commision, directory XII, project 2014, coordinater Dr. Dunker, for their financial suppor

LITERATURE

Mosier, S.A., Pierce, R.M., 1980, "Advanced Combustion Systems for Stationary Gas Turbine Engines", Vol. I, EPA Contract 68-02-2136.

Pierce, R.M., Smith, C.E., Hinton, B.S., 1990, "Advanced Combustion Systems for Stationary Gas Turbine Engines", Vol. III, EPA Contract 68-02-2136.

Shaw, R. J., Gilkey, S.,Hines, R., 1993, "Engine Technology Challenges for a 21st Century High Speed Civil Transport", ISABE 93-7064.

Zarzalis, N., Ripplinger, T.,1992, "NO Reduktion mittels der zweistufigen Verbrennung (Fett-Mager-Verbrennung) bei Gasturbinenbrennkammer", 1992, BWK, Bd 44, Nr 11.

Knapp, K., Meisel, J., Leuckel, W., Wittig, S., 1993, "Reduzierung der NOx-Emission in Gasturbinenbrennkammern durcb zweistufigen Verbrennungsführung.", VDI-Berichte Nr 1090, pp. 587-594.

Griebel, P., Behrendt, T., Hassa, C., Lückerath, R., Bergmann, V., Stricker, W., Zarzalis, N., 1995, "Untersucbung eines atmosphärisceben Fett-Mager-Brennkammersektors für Flugtriebwerke", VDI-Bericbt 1193, pp. 589-596.

Lenze, M., 1994, "Experimentelle Untersuchung zum Fett-Mager-Verbrennungskonzept bei Triebwerk- spezifischen Randbedingungen", Diplomarbeit, EBI Karlsruhe.

Tuttle, J.H., Shisler, R.A., Mellor, A.M., 1974, "Nitrogen Dioxide Formation in Gasturbine Engines : Measurements and Measurement Methods", Combustion Science and Technology, Vol. 9, pp. 261-271.

Amsden, A.A., O'Rourke. P.J., Butler, T.D., 1989, "KIVA-II: A Computer Programm for Chemically Reactive Flows with Sprays", Los Alamos Laboratry report LA-11560-MS.

Zarzalis, N., 1995, Private Communication, MTU.

Migueis, C.E., Hassa, C., 1995, "Experimentelle und numeriscbe Untersuchung zur optimierung des Mischmoduls einer fett-mager gestuften Brennkammer" VDI-Bericht 1193, pp 581-588.